JOURNAL OF GEOPHYSICAL RESEARCH, VOL. 107, NO. D23, 4729, doi:10.1029/2002JD002197, 2002

# Surface emissivity retrieval from Digital Airborne Imaging Spectrometer data

José A. Sobrino and Juan C. Jiménez-Muñoz
Global Change Unit, Department of Thermodynamics, Faculty of Physics, University of Valencia, Burjassot, Spain

Jélila Labed-Nachbrand and Françoise Nerry
Groupe de Recherche en Télédétection et Radiométrie, Laboratoire des Sciences de l'Image, de l'Informatique et de la Télédétection, Illkirch, France

Received 12 February 2002; revised 23 April 2002; accepted 7 May 2002; published 14 December 2002.

[1] A study has been carried out on the most recent algorithms for the estimation of land surface emissivity (ε) using high-resolution data (Digital Airborne Imaging Spectrometer, DAIS) over the Rhine Valley (France) and Castilla La Mancha (Spain). Three published methods have been applied for extracting absolute spectral emissivity information from images recorded during the DAISEX experiment in 1999. They are NDVI Thresholds Method (NDVI$^{THM}$), Normalized Emissivity Method (NEM) and Temperature/Emissivity Separation (TES). These lather two methods were originally designed to work over geological surfaces. Five methods have been used for extracting relative spectral emissivity. They are temperature-independent spectral indices method (TISI), reference channel method (REF), emissivity normalization method (NOR), emissivity re-normalization method (RE), and alpha emissivity method (ALPHA), respectively. NDVI$^{THM}$ and NEM give the same absolute emissivity values with differences between 1% and 0.2% depending on the thermal channel considered, while NDVI$^{THM}$ and TES give the greatest differences, around 2%. The comparison with in situ values shows that NDVI$^{THM}$ gives the best results for vegetation plots, while NEM gives the best ones for bare soil and water plots. The TISI and NOR relative methods give the same relative emissivity values within less than 0.4%, in accordance with *Becker and Li*'s [1990] conclusion as regards the superiority of these methods compared to the others. *INDEX TERMS:* 3360 Meteorology and Atmospheric Dynamics: Remote sensing; 3359 Meteorology and Atmospheric Dynamics: Radiative processes; 3394 Meteorology and Atmospheric Dynamics: Instruments and techniques; 1610 Global Change: Atmosphere (0315, 0325); 1640 Global Change: Remote sensing; *KEYWORDS:* DAIS, DAISEX, absolute emissivity, relative emissivity

**Citation:** Sobrino, J. A., J. C. Jiménez-Muñoz, J. Labed-Nachbrand, and F. Nerry, Surface emissivity retrieval from Digital Airborne Imaging Spectrometer data, *J. Geophys. Res.*, *107*(D23), 4729, doi:10.1029/2002JD002197, 2002.

## 1. Introduction

[2] The recovery of land surface temperature and emissivity from thermal infrared remote sensing data is important for the study of water and energy balances, climate models, lithological mapping and resource exploration, among others. However, two main problems must be solved in order to obtain the surface temperature and emissivity from thermal infrared data. First, the at-sensor radiances are affected by the contribution of the atmosphere, which results from absorption and reemission by atmospheric gases, mainly water vapor in the infrared domain of the electromagnetic spectrum. Thus, to access the at-surface radiances, atmospheric correction has to be performed through the use of a radiative transfer model. Second, the underdetermined nature of the thermal measurements, in which temperature and emissivity are coupled. If the thermal radiation is measured in N spectral channels, there will be N + 1 unknowns: N emissivities (one per channel) and a single surface temperature. The estimation of emissivity and temperature in multispectral thermal infrared data needs additional assumptions to resolve the indetermination. Assumptions are often related to laboratory or field emissivity measurements.

[3] Many papers, as mentioned below, have developed algorithms to extract surface parameters from IR data but relatively few papers have dealt with the comparison of the different published methods on surface emissivity estimation from actual remotely sensed data. In this paper we will focus our study on the comparison between recent algorithms for the estimation of land surface emissivity using data collected from thermal infrared multispectral DAIS (Digital Airborne Imaging Spectrometer) data acquired over the Barrax (Spain) and Colmar/Hartheim (France) test sites in the DAISEX (Digital Airborne Imaging Spectrometer Experiment) campaigns framework.

0148-0227/02/2002JD002197$09.00

**Table 1a.** Spectrometer Characteristics of the DAIS-7915 Sensor

| | Spectrometer Characteristics | | |
|---|---|---|---|
| Wavelength Range | Number of Bands | Bandwidth | Detector |
| 450–1050 nm | 32 | 25 nm | Si |
| 1500–1800 nm | 8 | 45 nm | InSb |
| 1900–2450 nm | 32 | 25 nm | InSb |
| 3000–5000 nm | 1 | 2.0 µm | MCT |
| 8700–12700 nm | 6[a] | 0.9 µm | MCT |

[a] Effective wavelengths for the six DAIS thermal channels: 8.747 µm (Channel 74), 9.648 µm (Channel 75), 10.482 µm (Channel 76), 11.266 µm (Channel 77), 11.997 µm (Channel 78), and 12.668 µm (Channel 79).

[4] Three methods have been applied to obtain absolute spectral emissivity and five methods have been applied to extract relative emissivity spectra. They are respectively the NDVI Thresolds Method (NDVI$^{\mathrm{THM}}$) [*Sobrino et al.*, 2001], Normalized Emissivity Method (NEM) [*Gillespie*, 1985] and Temperature/Emissivity Separation method (TES) [*Gillespie et al.*, 1999] for absolute emissivity, and Temperature-Indpendent Spectral Indices method (TISI) [*Becker and Li.*, 1990], REFerence channel method (REF) [*Kahle et al.*, 1980], emissivity NORmalization method (NOR) [*Gillespie*, 1985], emissivity RE-normalization method (RE) [*Stoll*, 1993], and ALPHA emissivity method (ALPHA) [*Kealy and Gabell*, 1990] for relative emissivity. The reference channel used to calculate DAIS relative emissivity values is the one centered at 10.482 µm (channel 76), and a maximum emissivity value of 0.98 has been arbitrarily chosen. After giving a description of the field campaign and reminding the principles of the methods used, a discussion and validation of the results is given.

## 2. Description of the DAISEX Campaign

[5] Since the mid 1980s the European Space Agency (ESA) has been involved in airborne campaigns and other studies aimed at developing the potential of spaceborne imaging spectroscopy for a range of different scientific applications. The latest of these activities, DAISEX, involved simultaneous data acquisitions using three different airborne imaging spectrometers (DAIS-7915, HyMap and POLDER) over test sites in southeast Spain and the Upper Rhine Valley (France).

### 2.1. DAIS Sensor

[6] DAIS-7915 or DAIS since spring 1995 is operated at the DLR (Deutsches Zentrum für Luft- und Raumfahrt) research center Oberpfaffenhofen, Germany. The 79-band imaging spectrometer was built by GER Corp. and funded by the European Union and DLR. The sensor covers the electromagnetic spectrum from the visible to the thermal infrared region with 4 individual spectrometers and a single band in the 3–5 µm region (see Tables 1a and 1b). At a 64-degree field of view (FOV) 512 pixels are recorded per scan line as well as 16 samples of each of the two external reference blackbodies. In an additional channel a set of auxiliary data including scan frequency line and facet counters and blackbody temperatures are stored. For later geometric correction roll, pitch and yaw information from two gyroscopes is recorded. Image data are recorded with a radiometric resolution of 15 bits per pixel and co-registered bands. All data are 16 bit encoded and stored in BIL format on Exabyte tape. More details about DAIS characteristics are given by *Müller et al.* [2001] and *Müller and Hausold* [2001].

[7] The DAIS sensor was installed on board the DLR-own DO228 aircraft, and the images were acquired on 17 July 1999 for Colmar/Harteim site and on 3–4 June 1999 for Barrax site (see Table 3).

### 2.2. Geometric and Atmospheric Correction

[8] DAIS images were geometric and atmospherically corrected by DLR as a part of the pre-processing of DAIS [*Richter*, 2000]. The geometry of airborne optical scanner data is subject to distortions caused by sensor movements during data acquisition. As these movements may be different from those of the aircraft (e.g., with sensors mounted on a stabilizing platform) the auxiliary data have to refer strictly to the sensor. The permanently changing viewing geometry within one flight line can only be embraced by a parametric approach as realized by the IDL-based software package PARGE (PARametric Geocoding) which was developed by D. Schläpfer, University of Zürich, RSL. Geocoding of DAIS data within the DAISEX project was done with this software [*Hausold*, 2001]. Moreover, an atmospheric correction methodology for imaging spectrometer data [*Richter*, 2001] was applied for DAIS using local atmospheric measurements as inputs of the MODTRAN radiative transfer code [*Berk et al.*, 1989].

### 2.3. Colmar/Harteim and Barrax Test Sites

[9] The Colmar (48°4′N; 7°20′E) and Harteim (47°57′N; 7°37′E) test sites are situated in the Upper Rhine Valley. The Upper Rhine Valley extends, roughly North-South, over 200 km from Basel, Switzerland (South) to Karlsruhe, Germany (North) and over approximately 80 km from the Vosges (West) to Black Forest (East). It is highly uniform flat plain, at an altitude of 250 m above sea level at the Southern end, down to 100 m at the Northern end. Its hydrology is characterized by the connection between the mountainous basins and the river and the presence of a large water table, one of the most important in Europe. The orientation of the Upper Rhine Valley has an impact on the regional atmospheric circulation and ventilation. Thus, the Upper Rhine Valley "Regio" represents a very interesting extended site for environmental and climate studies. The Colmar site is an agricultural experimental area operated by INRA (Institut National de Recherches Agronomiques), situated South of the city. The site includes experimental test fields with a variety of crops and experimental vineyards. The Harteim

**Table 1b.** Geometric and Radiometric Parameters of the DAIS-7915 Sensor

| Parameter | Value |
|---|---|
| | *Geometric Parameters* |
| IFOV | 3.3 mrad |
| Swath angle | ±26 degrees |
| Image pixels per line | 512 |
| Spatial Resolution | 2–20 m (depending on the flight altitude) |
| | *Radiometric Parameters* |
| Sensibility | |
| VIS/NIR | NER < 0.025 mW/cm$^2$ sr µm |
| SWIR | NER < 0.025 mW/cm$^2$ sr µm |
| MIR/TIR | NET < 0.1 K |
| Dynamic Range | 15 bit (no gain settings) |

site is a coniferous forest (*pinus sylvestrus*), about 40 years old, located 20 km Southwest of Freiburg (Germany). The extension of the forest is about 10 km North-South and 1.5 km East-West. In the middle, an experimental study area, run by the Meteorological Institute of the University of Freiburg, includes two towers instrumented for radiation and energy fluxes measurements within and above the canopy [*Nerry and Stoll*, 2001].

[10] The DAISEX campaigns in Spain have been carried out in the area of La Mancha, a plateau located at 700 m above the sea level (39°2′N, 2°10′W). The selection of Barrax as one of the test sites for the DAISEX experiment was not random, but justified through a large experience in using this area as test site for many previous remote sensing experiments. The Barrax site is situated in the West of the province of Albacete, 28 km from the capital town (39°3′N, 2°6′W). The dominant cultivation in the 10,000 ha area is approximately 65% dry land (of which 67% are winter cereals and 33% fallow land) and 35% irrigated land (corn 75%; barley/sunflower 15%; alfalfa 5%; onions 2.9%; vegetables 2.1%). Moreover, the University of Castilla-La Mancha, through the "Escuela Técnica Superior de Ingenieros Agrónomos," operates three agro-meteorological stations in the study area of Barrax [*Moreno et al.*, 2001].

### 2.4. Surface Radiometric Measurements

[11] Surface radiometric measurements were collected at the Colmar and Harteim sub-sites of the Upper Rhine Valley site, mostly during day 198 (17 July, 1999), which corresponds to the day when airborne acquisitions took place. Test surfaces used for the ground measurements include the following: (1) at the Colmar site, sugar beet, corn, fallow, potatoes, bare soil, car parking; and (2) at the Harteim site, pine (*pinus sylvestris*) forest. In the Thermal Infrared domain, various instruments were used that include fixed FOV-single band or multiband radiometers, and an imaging system (TIR camera). In addition, black bodies for calibration purposes. The instrumentation details are given in Table 2. The measurements used to estimate the TIR band emissivities of the different surfaces are from the CIMEL radiometer and the method used is the "reference channel method" [*Nerry et al.*, 2001].

[12] Instrumentation used for Barrax site is similar to the one used for Colmar and Harteim sites, with the addition of the OMEGA OS86 radiometer with 1 spectral band in the 8–14 μm range and a field of view (FOV) of 2°. Emissivity values have been performed over different targets (bare soil, nonirrigated barley and alfalfa) by the box method [*Alonso et al.*, 2001]. All measurements have been carried out simultaneously with the overflight of the DAIS sensor.

**Table 2.** Thermal Infrared Instrument Characteristics

| Model | Spectral Bands | Accuracy[a] | FOV |
|---|---|---|---|
| Barnes PRT5 | 10.5–12.5 μm | 0.1°C | 2° |
| GRTRad | 3.5–4.1 μm | 0.5°C | 4° |
| GRTRad | 9.9–11.4 μm | 0.1°C | 4° |
| GRTRad | 11.3–12.4 μm | 0.1°C | 4° |
| Cimel CE 312 | 8–13 μm | 0.1°C | 10° |
| Cimel CE 312 | 8.2–9.2 μm | 0.1°C | 10° |
| Cimel CE 312 | 10.3–11.3 μm | 0.1°C | 10° |
| Cimel CE 312 | 11.5–12.5 μm | 0.1°C | 10° |
| Everest 3000.3LC | 8–14 μm | 0.2°C | 25° |
| Everest 3000.4ZLC | 8–14 μm | 0.2°C | 15° |
| Everest 3000.4ZLC | 8–14 μm | 0.2°C | 4° |
| Raytek | 8–14 μm | 0.2°C | 8° |
| AGA Thermo Vision 782 | 8–14 μm | | 7°, 20° |

[a] According to the manufacturer's documentation.

**Table 3.** DAIS Images Used to Obtain Absolute and Relative Spectral Emissivity for the Barrax Site

| Image | Flight | Date | GMT |
|---|---|---|---|
| 1 | 1 | 03-06-1999 | 11:53 |
| 2 | 2 | 03-06-1999 | 12:09 |
| 3 | 1 | 04-06-1999 | 08:02 |
| 4 | 2 | 04-06-1999 | 08:17 |
| 5 | 1 | 04-06-1999 | 15:00 |
| 6 | 2 | 04-06-1999 | 15:13 |

## 3. Emissivity Methods

[13] A brief description of each method used to calculate absolute and relative spectral emissivity is given hereafter. The term "absolute emissivity" refers to the absolute value of this quantity, which is very important for surface temperature estimations. The term "relative emissivity" refers to the value of emissivity with respect to another emissivity reference value. In this case, the absolute value of the emissivity can not be obtained but it is possible to recover the shape of the emissivity spectrum for the different targets. This data can be used for classification methods. The term "spectral" in both cases has been used to mark that the emissivity values have been obtained for different DAIS thermal channels (from 74 to 79). More details about the methods involved in this paper can be found in the references given at sections 3.1 and 3.2.

### 3.1. Absolute Spectral Emissivity

[14] In order to extract absolute spectral emissivity three methods have been considered. They are described below.

**Figure 1.** Plots used to extract absolute and relative emissivity from the Barrax site according to DAISEX notation: Bare Soil (S10), Alfalfa (V16), Corn-two leaves (SV1), Nonirrigated Barley (V25) and Water (W).

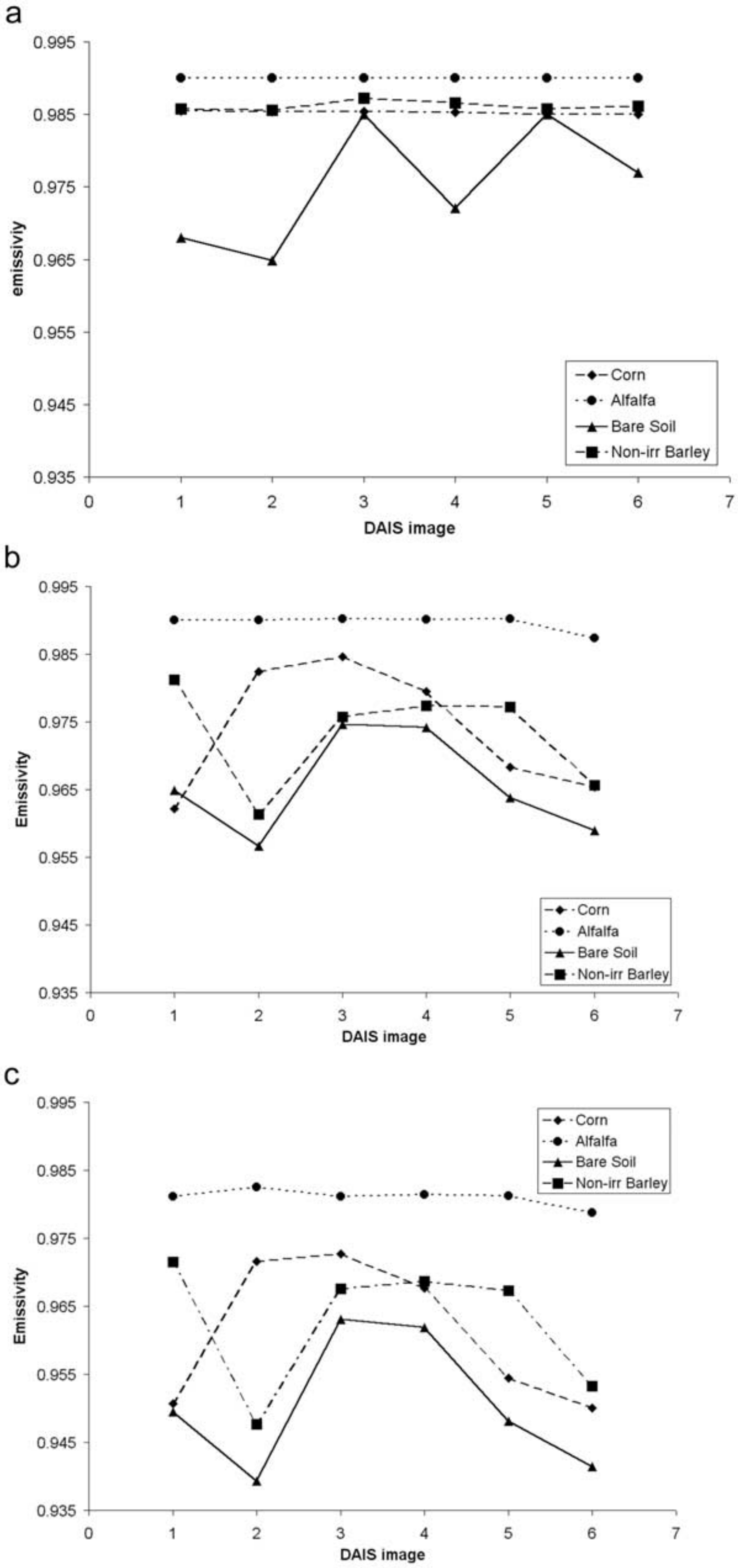

**Figure 2.** Absolute emissivity for the six DAIS images acquired over Barrax site in 1999 (see Table 3) extracted from DAIS thermal channel 77 (11.266 μm) for Corn-two leaves, Alfalfa, Bare Soil and Nonirrigated Barley using (a) the NDVI$^{THM}$, (b) the NEM and (c) the TES methods.

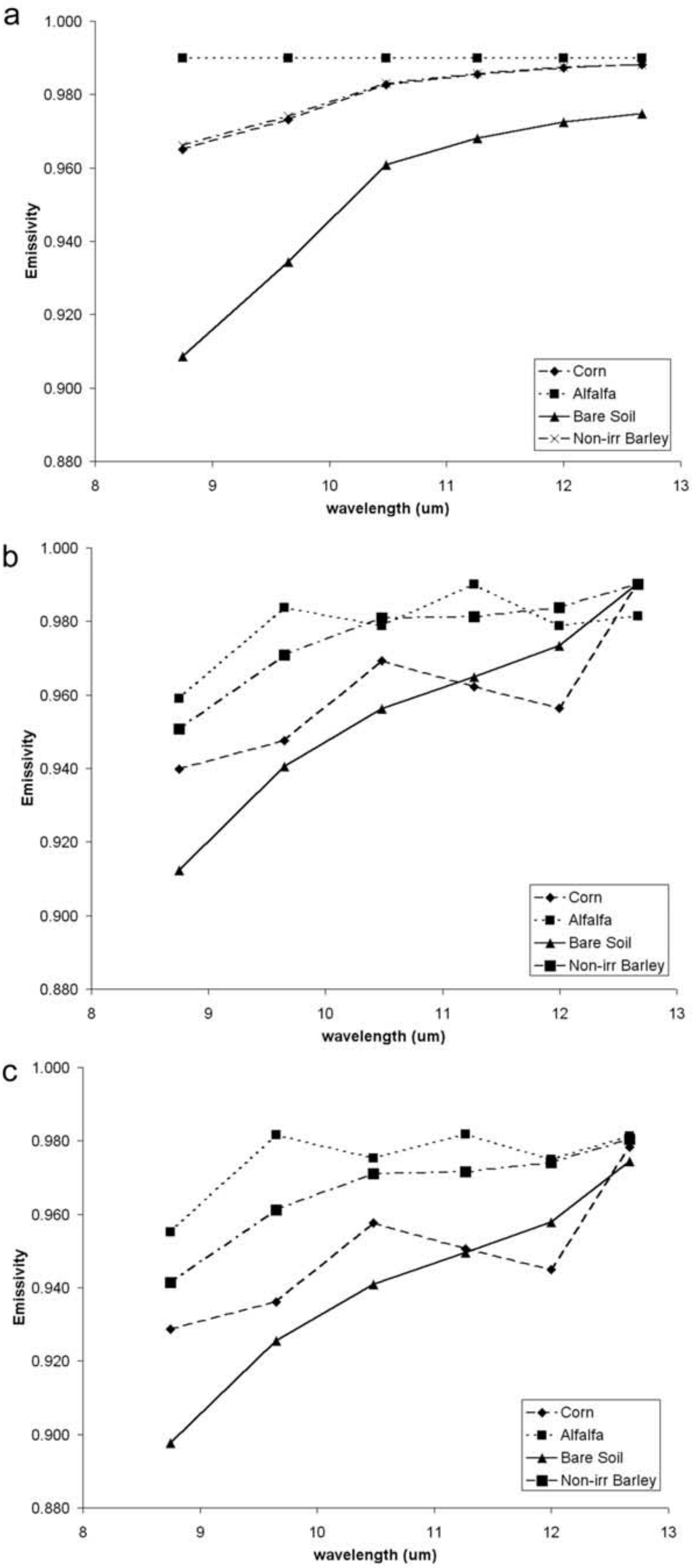

**Figure 3.** Absolute spectral emissivity for different plots from the Barrax site (6 June 1999; solar noon) obtained with (a) the $NDVI^{THM}$, (b) the NEM and (c) the TES methods.

### 3.1.1. NDVI Thresholds Method (NDVI$^{THM}$)

[15] It is a simplified method based on the estimation of emissivity, $\varepsilon$, using atmospherically corrected data in the visible and near infrared channels [*Sobrino et al.*, 2001], which considers three different type of pixels depending on the NDVI value: bare soil pixels (NDVI < 0.2), mixed pixels ($0.2 \leq$ NDVI $\leq 0.5$) and fully vegetation pixels (NDVI > 0.5). The NDVI$^{THM}$ have been applied for NOAA channels 4 and 5 [*Sobrino*, 2000] and for MODIS channels [*El Kharraz*, 2001]. We have adapted this method to DAIS thermal channels 74 to 79 using the methodology proposed by *Sobrino* [2000] for rough and nonhomogenous surfaces with the help of Salisbury's spectra [*Salisbury and D'Aria*, 1992] and the DAIS filter functions to obtain the appropriate expressions to estimate absolute emissivity. The NDVI value have been calculated with the well-known equation that uses reflectivity values from the Red region ($\rho_{red}$) and Near InfraRred ($\rho_{nir}$) region, according to:

$$\mathrm{NDVI} = \frac{\rho_{red} - \rho_{nir}}{\rho_{red} + \rho_{nir}} \tag{1}$$

The DAIS channels 10 (0.659 $\mu$m) and 22 (0.868 $\mu$m) have been used for $\rho_{red}$ and $\rho_{nir}$ respectively. The final expressions obtained for this method are for bare soil pixels (NDVI < 0.2),

$$\varepsilon_{74} = -0.378\ \rho_{red} + 1.002 \tag{2a}$$

$$\varepsilon_{75} = -0.209\ \rho_{red} + 0.986 \tag{2b}$$

$$\varepsilon_{76} = -0.094\ \rho_{red} + 0.984 \tag{2c}$$

$$\varepsilon_{77} = -0.081\ \rho_{red} + 0.988 \tag{2d}$$

$$\varepsilon_{78} = -0.063\ \rho_{red} + 0.988 \tag{2e}$$

$$\varepsilon_{79} = -0.066\ \rho_{red} + 0.991 \tag{2f}$$

for mixed pixels ($0.2 \leq$ NDVI $\leq 0.5$),

$$\varepsilon_{74} = 0.963 + 0.025\ P_v \tag{3a}$$

$$\varepsilon_{75} = 0.972 + 0.016\ P_v \tag{3b}$$

$$\varepsilon_{76} = 0.982 + 0.008\ P_v \tag{3c}$$

$$\varepsilon_{77} = 0.985 + 0.006\ P_v \tag{3d}$$

$$\varepsilon_{78} = 0.987 + 0.004\ P_v \tag{3e}$$

$$\varepsilon_{79} = 0.988 + 0.002\ P_v \tag{3f}$$

and for vegetation pixels (NDVI > 0.5),

$$\varepsilon_{74} = \varepsilon_{75} = \varepsilon_{76} = \varepsilon_{77} = \varepsilon_{78} = \varepsilon_{79} = 0.990 \tag{4}$$

with $P_v$ being the vegetation proportion, given by

$$P_v = \frac{\mathrm{NDVI} - \mathrm{NDVI}_{min}}{(\mathrm{NDVI}_{max} - \mathrm{NDVI}_{min})^2} \tag{5}$$

**Table 4.** Difference of Absolute Emissivity Values Between the Three Methods (NDVI$^{THM}$, NEM, and TES) for Image 1 (6 June 1999; 11:53 Local Time) Acquired Over the Barrax Site

| | NDVI$^{THM}$-NEM | | NDVI$^{THM}$-TES | | NEM-TES | |
|---|---|---|---|---|---|---|
| Channel | Mean | Desv | Mean | Desv | Mean | Desv |
| 74 | 0.015 | 0.022 | 0.026 | 0.021 | 0.011 | 0.003 |
| 75 | 0.008 | 0.016 | 0.018 | 0.016 | 0.011 | 0.003 |
| 76 | 0.007 | 0.011 | 0.018 | 0.012 | 0.011 | 0.003 |
| 77 | 0.007 | 0.010 | 0.018 | 0.011 | 0.011 | 0.003 |
| 78 | 0.006 | 0.013 | 0.017 | 0.013 | 0.011 | 0.003 |
| 79 | −0.002 | 0.010 | 0.009 | 0.009 | 0.011 | 0.003 |

[16] The constraint of this method is that it cannot be used to extract water emissivity values because it is not possible to apply the NDVI and $P_v$ equations for water pixels.

### 3.1.2. Normalized Emissivity Method (NEM)

[17] With this method thermal images obtained from DAIS sensor are inverted to extract an emissivity value for every pixel image and for every thermal DAIS channel. Using this method, some iterations have been made until the downwelling radiance between two consecutive iterations reaches a convergence of 0.05 W m$^{-2}$ sr$^{-1}$ $\mu$m$^{-1}$. The method also needs an initial emissivity value to recalculate the final emissivities. In our case, we have made only one iteration, and we have chosen an initial emissivity value of 0.99. Note that this method is similar to the NOR method shown in the next section, with the iterative process being the difference between both methods.

### 3.1.3. Temperature/Emissivity Separation Method (TES)

[18] The TES algorithm uses the NEM to estimate temperature, from which emissivity ratios are calculated. These ratio values are the NEM emissivities normalized by their average value. The ratio spectrum preserves the shape, but not the amplitude, of the actual emissivities. To recover the amplitude, and hence a refined estimate of the temperature, the spectral contrast (MMD) is calculated and used to predict the minimum emissivity. For this purpose, the Salisbury's spectra with the DAIS filter functions have been used to obtain the following equation with a correlation coefficient of 0.996:

$$\varepsilon_{min} = 0.9843 - 1.0616\ \mathrm{MMD}\ (\mathrm{correlation} : 0.9956) \tag{6}$$

A similar expression for $\varepsilon_{min}$ and MMD is given by *Gillespie et al.* [1999] for ASTER sensor onboard NASA's TERRA satellite. Equation (6) is used to calculate TES emissivities for DAIS thermal channels.

[19] Due to the fact that the downwelling radiances are known (using the radio soundings as input data in the MODTRAN code and executing it in thermal radiance mode) we only require one iteration when applying the NEM and TES methods. Furthermore the initial emissivity value selection is not very relevant, the values differ only by 0.001 by choosing 0.98 or NDVI emissivity as initial emissivity. The reader interested in a more detailed study of the NEM and TES methods can consult *Gillespie et al.* [1999].

## 3.2. Relative Spectral Emissivity

[20] Next, we are going to summarize the methods compared in the present paper for extracting relative spectral emissivity values. For more details on the different

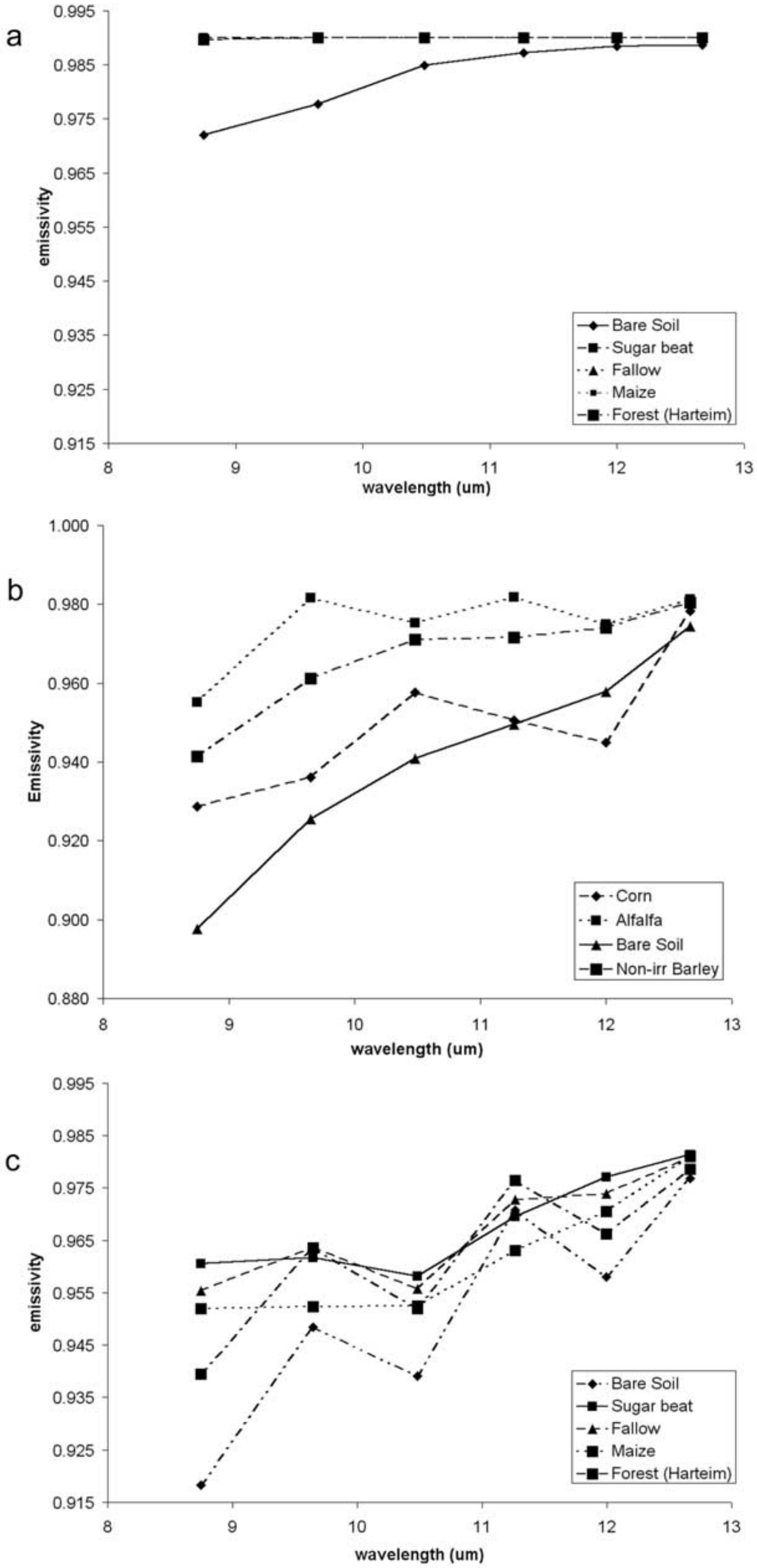

**Figure 4.** Absolute spectral emissivity for different plots from Colmar (0931 UTC) and Harteim (0917 UTC) sites obtained with (a) the NDVI$^{THM}$, (b) the NEM and (c) the TES methods.

**Table 5.** Comparison Between Emissivity Values Obtained With the Different Methods and Those Obtained With the In Situ Measurements for the Thermal Infrared Region (8–14 μm) and for Image 1[a]

| Method | Plot | $\varepsilon_{\text{method}}$ | $\varepsilon_{\text{in situ}}$ | $\varepsilon_{\text{meth}}$-$\varepsilon_{\text{situ}}$ | Error, % |
|---|---|---|---|---|---|
| NDVI | Corn | 0.980 | 0.974 | 0.006 | 0.62 |
| NDVI | Alfalfa | 0.990 | 0.996 | −0.006 | 0.60 |
| NDVI | Bare Soil | 0.950 | 0.966 | −0.016 | 1.66 |
| NDVI | Barley | 0.980 | 0.970 | 0.010 | 1.03 |
| NDVI | Water | – | 0.987 | – | – |
| NEM | Corn | 0.959 | 0.974 | −0.015 | 1.54 |
| NEM | Alfalfa | 0.980 | 0.996 | −0.016 | 1.61 |
| NEM | Bare Soil | 0.955 | 0.966 | −0.011 | 1.14 |
| NEM | Barley | 0.977 | 0.970 | 0.007 | 0.72 |
| NEM | Water | 0.983 | 0.987 | −0.004 | 0.41 |
| TES | Corn | 0.948 | 0.974 | −0.026 | 2.67 |
| TES | Alfalfa | 0.971 | 0.996 | −0.025 | 2.51 |
| TES | Bare Soil | 0.940 | 0.966 | −0.026 | 2.69 |
| TES | Barley | 0.967 | 0.970 | −0.003 | 0.31 |
| TES | Water | 0.976 | 0.987 | −0.011 | 1.11 |

[a] See Table 3. For the NDVI method, mean = 0.98, σ = 0.49, and rms = 1.09; for the NEM method, mean = 1.08, σ = 0.52, and rms = 1.20; and for the TES method, mean = 1.86, σ = 1.09, and rms = 2.15 (values refer to the error in percent).

methods the readers can refer to *Li et al.* [1999] and *Sobrino et al.* [2001]. They are as follows:

1. In the $\text{TISI}_{\text{ir}}$ method [*Becker and Li*, 1990], the TISI for two channels i and r is defined from a ratio of channel radiances. The channel having the highest surface brightness temperature among N is chosen to be the reference channel, r.
2. The REF method [*Kahle et al.*, 1980], also called the Model Emissivity method, assumes that the emissivity in channel r is constant for all pixels. An approximate surface temperature is then derived from atmospherically corrected radiances and used to retrieve the emissivity values for the remaining channels.
3. The NOR method [*Gillespie*, 1985] assumes a constant emissivity in all N channels for a given pixel, which enables N temperatures to be calculated, the maximum of which is considered to be the Land Surface Temperature. Deriving emissivity values for the other channels is then achieved as for the REF method.
4. The RE method [*Stoll*, 1993] is similar to the two-channel TISI method, but involves a simple ratio of channel emissivities.
5. The ALPHA technique [*Kealy and Gabell*, 1990] is based on Wien's approximation of the Planck function. Taking the natural logarithm of the approximated radiance and eliminating the surface temperature when considering the equation for one channel and the one representing the mean for N channels, the alpha coefficient is shown to be directly obtained from the measured radiance.

## 4. Results and Validation

[21] In this section, we will show the results obtained applying the different methods to DAIS images. For this purpose, we have worked with boxes of 4 × 4 pixels to extract an average emissivity value. For the Barrax site six images have been considered (see Table 3), with the following selected plots: corn (two leaves), bare soil, alfalfa, non-irrigated barley and water (see Figure 1). For the Colmar/Hartheim sites, only two images (one for each location) were available and respectively recorded at 09:31 UTC and 09:17 UTC, on 17 July 1999. Four samples were considered over the Colmar area (bare soil, sugar beet, fallow and maize) whereas forest was studied over the Hartheim site.

### 4.1. Comparison of Absolute Emissivity Methods

[22] Taking into account the six images acquired over the Barrax site, we can give a temporal evolution for the different emissivity values obtained with $\text{NDVI}^{\text{THM}}$, NEM and TES methods for the different plots. Figure 2 shows the temporal evolution using the DAIS thermal channel 77 (11.266 μm). In this figure it can be seen that alfalfa has the highest values of emissivity, while bare soil has the lowest. It also shows that NEM and TES methods give similar values of absolute emissivity. The $\text{NDVI}^{\text{THM}}$ gives higher values. This is due to the $\text{NDVI}^{\text{THM}}$ methodology, in which different zones are classified according to their NDVI value. For NDVI values grater than 0.5 these zones are considered as vegetation, with an emissivity value of 0.99 for all the thermal channels (see equation (4)). It is therefore possible that some zones have an overestimation value of emissivity. The figure also highlights that the $\text{NDVI}^{\text{THM}}$ gives constant results over this period of time. Using the NEM and the TES method for alfalfa, similar behavior was recorded; however, the values for the other plots change over the period.

[23] Figure 3 shows the absolute spectral emissivities obtained for the Barrax site with the different methods on 3 June 1999. It is evident that the NEM and TES methods

**Figure 5.** Absolute emissivity image obtained from DAIS data acquired on 6-June, 1999 at 11:53 local time for the Barrax site (image 1 according to Table 3), using a $\text{NDVI}^{\text{THM}}$/NEM combination method.

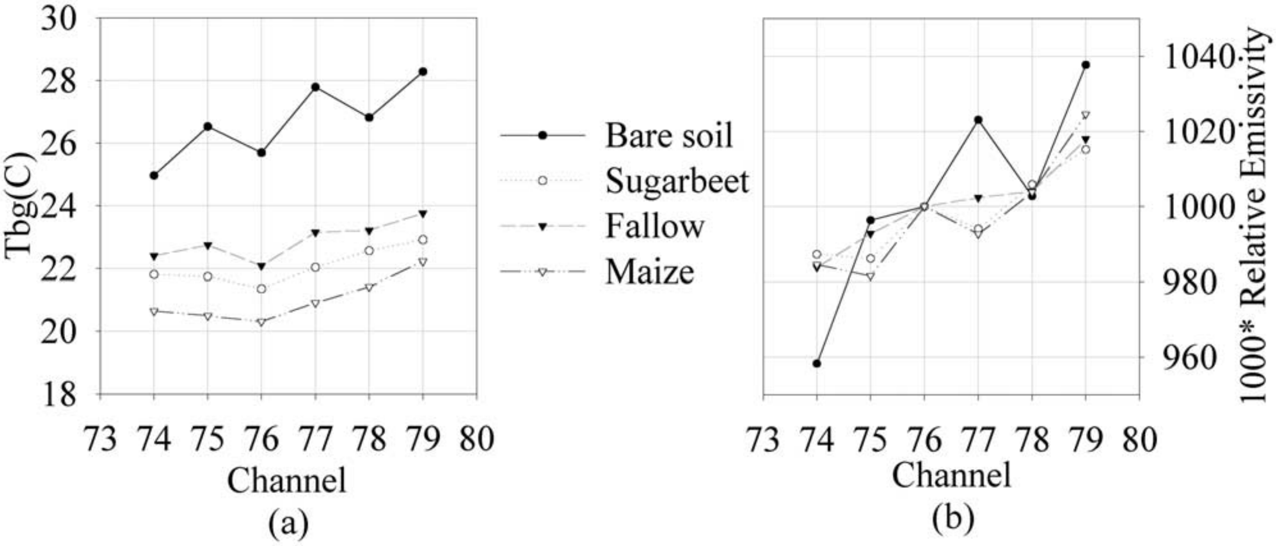

**Figure 6.** (a) Plot of the brightness temperature at ground level versus de DAIS channels and (b) plot of the REF method for different samples.

give similar emissivity values. Similar conclusions can be extracted for other images. An estimation of the differences between the values obtained with the three methods for the Barrax site and for every DAIS thermal channel can be found in Table 4. This table clearly shows that NDVI$^{THM}$ and TES methods give the greater differences, and the NDVI$^{THM}$ and NEM, give the lowest. Moreover, these differences depend on the channel considered. However for NEM and TES methods a constant difference of around 1% between the emissivity values for all the channels was obtained. The spectral variations showed in Figure 3 for each plot, particularly for corn and barley, can be explained taking into account the mixture of vegetation (high emissivity values) and bare soil (low emissivity values).

[24] Regarding the Colmar and Harteim sites, Figure 4 depicts the absolute emissivities obtained with the different methods. The five graphs show a slight increase in wavelength. Bare soil emissivity values display lower but larger variation in wavelength. Sugar beet and maize show a relatively high emissivity value. Fallow and bare soil showed parallel behavior but with bare soil having low emissivity values. This is due to the large proportion of bare soil present in the fallow. Qualitatively, the dispersion of emissivity values is within 2–3%, the lesser discrepancy being observed at 12.67 μm (channel 79).

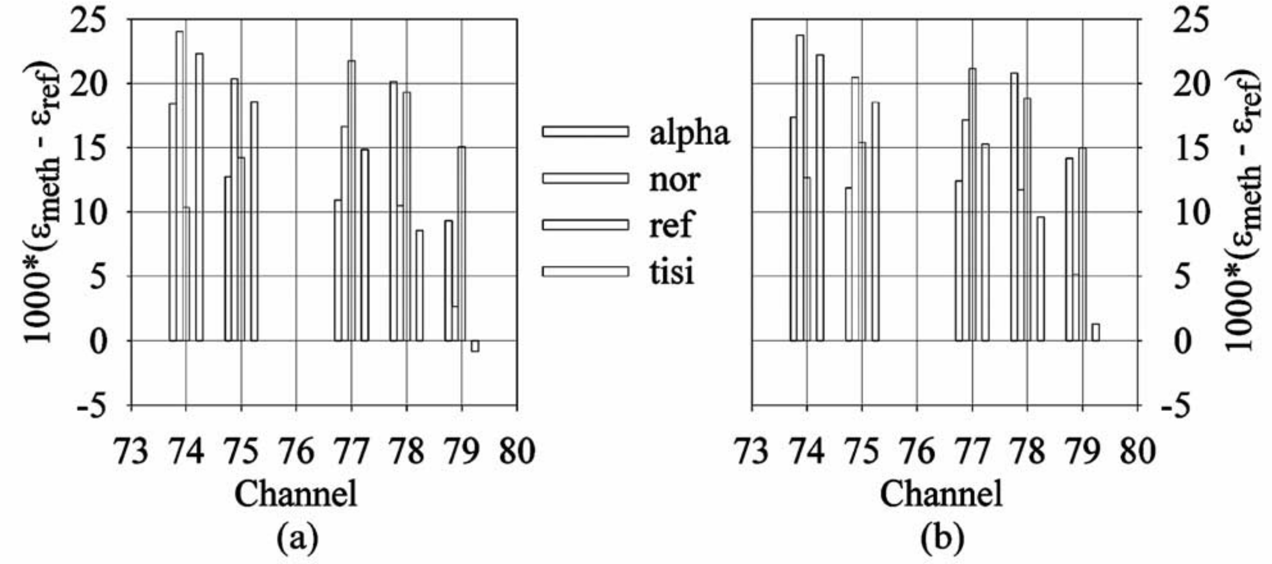

**Figure 7.** (a) Plot of the difference between the methods against the REF method for bare soil (Colmar) and (b) plot of the difference between the five methods against the REF method for forest (Hartheim). For each channel, left to right, bars represent ALPHA, NOR, REF, and TISI.

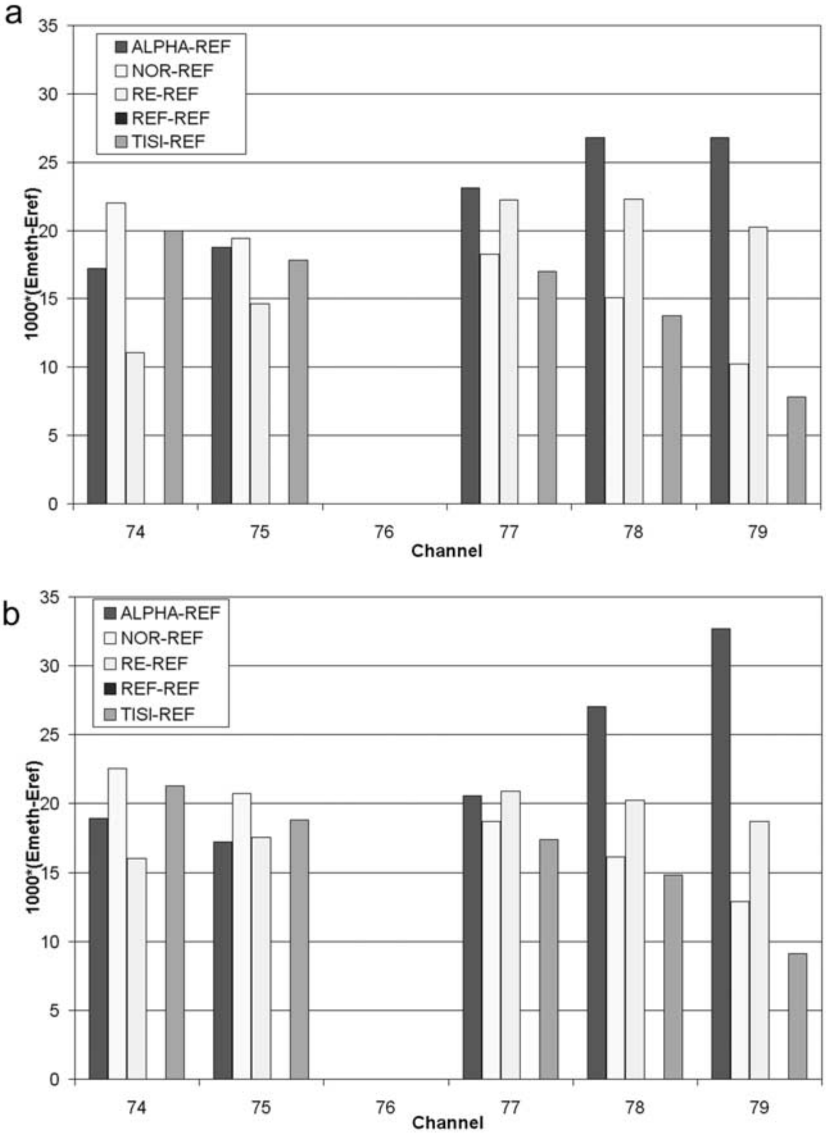

**Figure 8.** Plot of the difference between the five relative emissivity methods against the REF method for (a) Bare Soil and (b) Alfalfa (Barrax site, 3 June 1999, 11:53 local time). For each channel, left to right, bars represent ALPHA, NOR, RE, REF and TISI.

[25] The best way to check the validity of these methods is to compare them with the in situ measurements. For absolute emissivity values, in situ measurements were carried out only for the Barrax site. These emissivities were measured using the box method [*Nerry et al.*, 1990] with the Raytek field radiometer working in the 8–14 μm (see Table 2).

[26] In situ values are compared with those obtained for DAIS images with the different methods using DAIS thermal channel 77 (11.266 μm), which has a similar effective wavelength as that for the field radiometer (≈11 μm). However, it is more precise to consider all the DAIS thermal infared (TIR) channels values and to calculate a mean value using the following equation:

$$\langle\varepsilon\rangle_{\mathrm{TIR}} = \langle\varepsilon\rangle^{\mathrm{DAIS}}_{74-79} = \frac{1}{\Delta\lambda}\int_{\lambda_{74}}^{\lambda_{79}} \varepsilon_\lambda \mathrm{dl} \qquad (7)$$

[27] Table 5 shows the comparison between emissivity in situ values and the emissivity values extracted from DAIS images using equation (7) with the different methods. The error given here has been calculated from the following:

$$\mathrm{Error}(\%) = \frac{|\varepsilon_{\mathrm{method}} - \varepsilon_{\mathrm{in\ situ}}|}{\varepsilon_{\mathrm{in\ situ}}} \times 100 \qquad (8)$$

[28] The best results for NDVI$^{\mathrm{THM}}$ and NEM methods are obtained, with an error of around 1%. A more detailed study of the results obtained shows that the NDVI$^{\mathrm{THM}}$ gives the best results for corn and alfalfa, while NEM for bare soil and water plots and TES method for nonirrigated barley plot.

[29] Taking into account that the NDVI$^{\mathrm{THM}}$ gives the best results for plots with high NDVI values and the NEM is the best method for plots with low NDVI values, a mixed

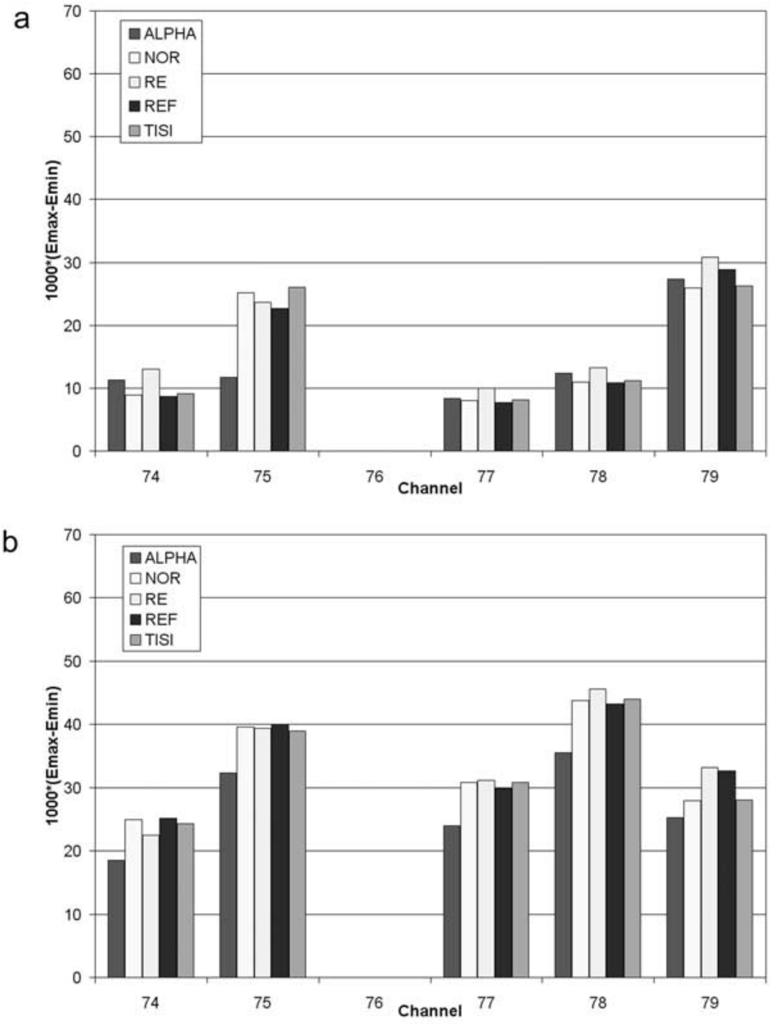

**Figure 9.** Difference between the maximum and minimum emissivity for all the DAIS images and for every relative method considering different zones: (a) Bare Soil, (b) Corn-two leaves, (c) Alfalfa and (d) Nonirrigated Barley. For each channel, left to right, bars represent: ALPHA, NOR, RE, REF and TISI.

method depending on the NDVI values is proposed using the following: If NDVI < 0.2, NEM is proposed; if $0.2 \leq \mathrm{NDVI} \leq 0.5$, $\mathrm{NDVI}^{\mathrm{THM}}$ (see equations (3a)–(3f)); and if NDVI > 0.5, a constant value is assumed, $\varepsilon = 0.990$.

[30] With this methodology we can obtain an emissivity image from DAIS sensor with more accurate values (see Figure 5).

### 4.2. Comparison of Relative Emissivity Methods

[31] The relative emissivity values have been calculated against the emissivity in channel 76 (central wavelength: 10.482 μm) chosen as the reference channel with a maximum value of 0.98. For the three sites and the different samples considered (bare soil, three vegetation types, forest, etc…) a general trend is observed on the average of 4 × 4 pixels values on the same type of surface for the Barrax, Colmar and Hartheim sites.

1. The global variation of the relative emissivity, considering all samples, reaches 5 to 7% and the spectral behavior of the emissivity signatures follow the behavior of the brightness temperature at ground level (as shown on Figure 6). This behavior might be due to an intercalibration problem of the DAIS channels and not to an actual spectral characteristic of the samples.

2. The REF method gives the lowest relative emissivity values (about 2% less than the other methods): approximate surface temperature derived from atmospherically corrected radiances in reference channel 76 is obviously overestimated and therefore the retrieved emissivity values for the remaining channels are underestimated.

3. The ALPHA method shows results similar to those obtained with the other methods, thus departing from theory: as the contribution of the downwelling radiation is neglected in constructing the ALPHA spectral index, this method is supposed to give different results from the others. The results aim to indicate the impact of the downwelling radiation is negligible.

4. Taking the values given by the REF method as reference, the differences between the methods strongly depend on both the sample and the channel considered as pointed out in the histograms of bare soil, forest and alfalfa drawn on Figures 7 and 8, as an example.

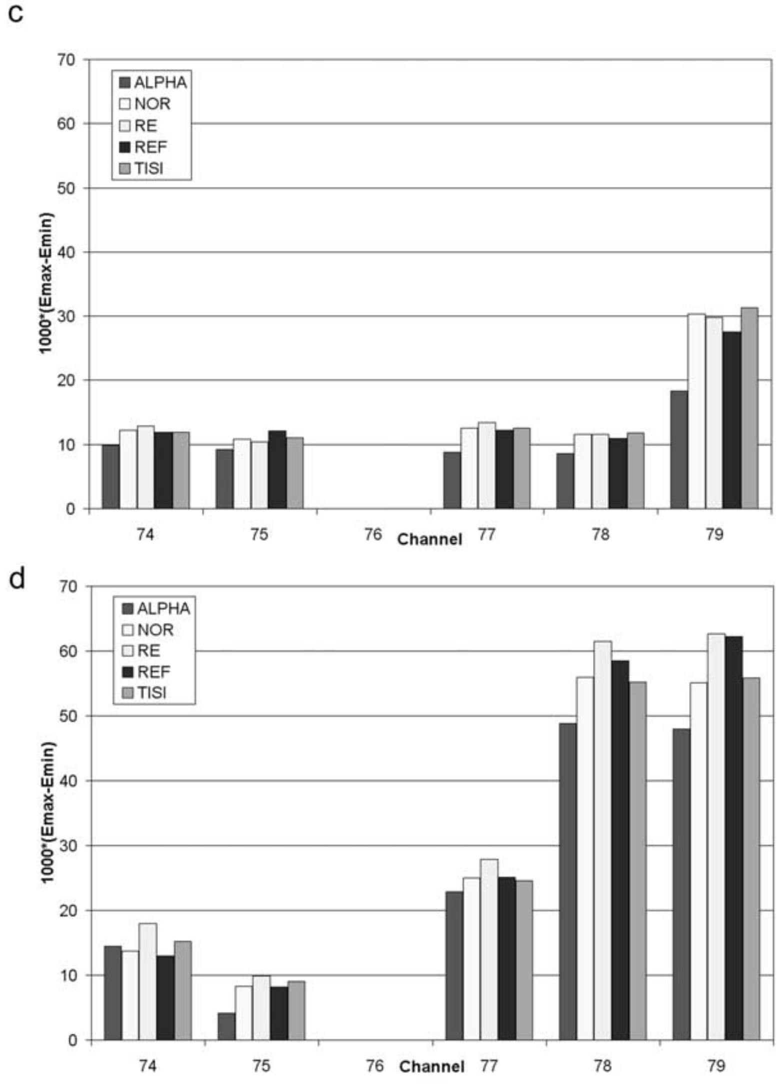

**Figure 9.** (continued)

[32] TISI and NOR methods give slightly the same difference against the REF method in accordance with Becker and Li's conclusion as regards the superiority of these both methods compared to the others.

[33] Taking into account these relative methods, it is possible to make a study of the temporal variation of relative emissivity over the Barrax data. For this purpose, we calculate the difference between the maximum emissivity and the minimum emissivity. The results can be observed in Figure 9.

[34] It can be seen that channel 79 normally gives the highest amplitude, while channels 74 and 77 give the lowest. Therefore, these channels are the most appropriate to study emissivity. This result may be due to the high atmosphere transmissivity for the DAIS channel 77.

### 4.3. Spectral Contrast

[35] We have given the name 'spectral contrast' to the image showing the difference between maximum and minimum emissivity. Figure 10 shows the spectral contrast obtained with the TISI method for the Barrax and Colmar test sites. It is evident that the spectral contrast is low for fully vegetated covers and larger for bare soils. Minimum emissivities are usually found for the low wavelength channel (i.e., channel 74, 8.8 μm), and maximum for channels 76–79, with small variations among these channels for a given surface type.

## 5. Conclusion

[36] This paper shows a comparison of various methods to obtain absolute and relative spectral emissivity from DAIS thermal channels 74 to 79. For absolute emissivity the NDVI$^{THM}$, the NEM and the TES methods have been used. We can observe that the NDVI$^{THM}$ gives the highest values for emissivity, while the NEM gives the lowest. The absolute emissivity differences for NDVI$^{THM}$ and NEM are around 1% and 0.2% depending on the DAIS thermal channel, 1% for NEM and TES, and approximately 2% for NDVI$^{THM}$ and TES. Comparing these results with the emissivities obtained in situ, it can be concluded that the NDVI$^{THM}$ gives the best results for vegetation plots and NEM for bare soil and water plots, with errors around 1% in both cases. Finally, it should be noted that this study has

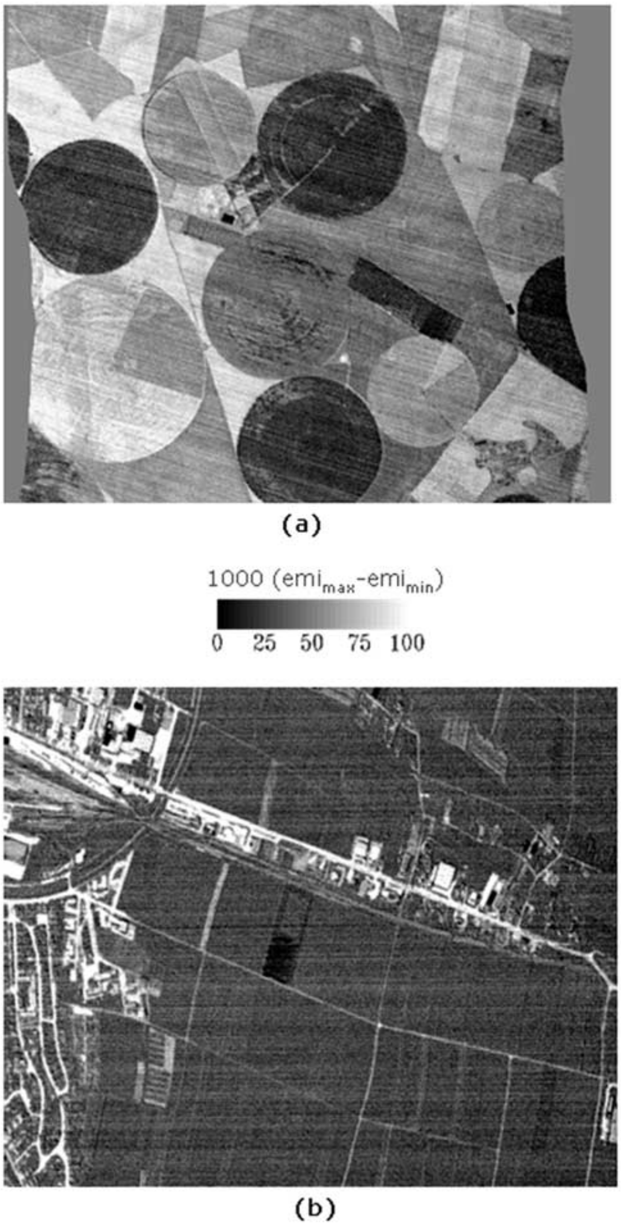

**Figure 10.** Image of maximum-minimum channel emissivity difference obtained with the TISI method for (a) Barrax, 3/6/99, BAR1; and (b) Colmar; 17/7/99, 9:32 UT.

been carried out over specific sites using data from a sensor onboard an aircraft. In the future we will carry out more extensive studies over different areas and using satellites images such as those given by ASTER. Of the five methods used for obtaining relative emissivity (TISI, NOR, REF, RE, ALPHA) it has been shown that TISI and NOR provide the best results.

[37] **Acknowledgments.** The authors wish to express their gratitude to J. Salisbury from the Johns Hopkins University (United States) for providing us with the spectral data set of bare soil reflectivity measurements in the band of 0.4–14 μm used in this paper. This research was supported in part by the European Union (WATERMED, Project ICA3-ct-1999-00015) and the European Space Agency ESA-ESTEC (DAISEX, Project 13390/NL/GD). The authors also wish to thank the German Aerospace Research Establishment (DLR) for providing the DAIS images. José Moreno (University of Valencia) is acknowledged for the coordination and compilation of the database.

## References

Alonso, L., et al., Surface radiometric measurements at Barrax, DAISEX Final Results Workshop, *NASA Spec. Publ., SP-499*, 71–77, 2001.

Becker, F., and Z.-L. Li, Temperature-independent spectral indices in thermal infrared bands, *Remote Sens. Environ.*, *32*, 17–33, 1990.

Berk, A., L. S. Bernstein, and D. C. Robertson, MODTRAN: A moderate resolution model for LOWTRAN 7, *Tech. Rep. GL-TR-89-0122*, Air Force Geophys. Lab., Bedford, Mass., 1989.

El Kharraz, J., Estimación de la Temperatura de la Superficie Terrestre y del contenido total en vapor de agua de la atmósfera a partir de datos MODIS, M. Sc., Univ. of Valencia, Valencia, Spain, 2001.

Gillespie, A. R., Lithologic mapping of silicate rocks using TIMS, in *The TIMS Data Users' Workshop*, *JPL Publ., 86-38*, 29–44, 1985.

Gillespie, A. R., S. Rokugawa, S. J. Hook, T. Matsunaga, and B. Kahle, Temperature/emissivity separation algorithm theoretical basis document, version 2.4, contract NAS5-31372, Natl. Aeronaut. and Space Admin., Washington, D. C., 1999.

Hausold, A., Geocoding methodology for imaging spectrometer data, in *DAISEX Final Results Workshop*, *Eur. Space Agency Spec. Publ., SP-499*, 91–96, 2001.

Kahle, A. B., D. P. Madura, and J. M. Soha, Middle infrared multispectral aircraft scanner data: analysis for geological applications, *Appl. Opt.*, *19*(14), 2279–2290, 1980.

Kealy, P. S., and A. R. Gabell, Estimation of emissivity and temperature using alpha coefficients, in *Proceedings of the Second TIMS Workshop*, *JPL Publ., 90-55*, 11–15, 1990.

Li, Z.-L., F. Becker, M. P. Stoll, and Z. Wan, Evaluation of six methods for extracting relative emissivity spectra from thermal infrared images, *Remote Sens. Environ.*, *69*, 197–214, 1999.

Moreno, J., A. Calera, V. Caselles, J. M. Cisneros, J. A. Martínez-Lozano, J. Meliá, F. Montero, and J. A. Sobrino, The measurement programme at Barrax, in *DAISEX Final Results Workshop*, *NASA Spec. Publ., SP-499*, 43–51, 2001.

Müller, A., and A. Hausold, The Airborne Spectrometer Data Acquisition Programme in 1998, 1999 and 2000, in *DAISEX Final Results Workshop*, *NASA Spec. Publ., SP-499*, 7–11, 2001.

Müller, A., P. Gege, and T. Cocks, The airborne imaging spectrometers used in DAISEX, in *DAISEX Final Results Workshop*, *NASA Spec. Publ., SP-499*, 3–6, 2001.

Nerry, F., and M. P. Stoll, The DAISEX'99 measurements program at Colmar/Harteim, in *DAISEX Final Results Workshop*, *NASA Spec. Publ., SP-499*, 25–30, 2001.

Nerry, F., J. Labed, and M. P. Stoll, Spectral properties of lands surfaces in the thermal infrared band, 2, Field method for spectrally averaged emissivity measurements, *J. Geophys. Res.*, *95*, 7045–7062, 1990.

Nerry, F., A. Leone, M. P. Stoll, M. Menenti, L. Jia, and J. A. Sobrino, Surface radiometric measurements at Colmar/Harteim, in *DAISEX Final Results Workshop*, *NASA Spec. Publ., SP-499*, 31–36, 2001.

Richter, R., Atmospheric/topographic correction for wide FOV airborne imagery: Model ATCOR4, *DLR Rep. DLR-IB 564-04/00*, Dtsch. Luft- und Raumfahrt, Wessling, Germany, 2000.

Richter, R., Atmospheric correction methodology for imaging spectrometer data, in *DAISEX Final Results Workshop*, *NASA Spec. Publ., SP-499*, 97–109, 2001.

Salisbury, J. W., and M. D'Aria, Emissivity of terrestrial materials in the 8–14 um atmospheric window, *Remote Sens. Environ.*, *42*, 83–106, 1992.

Sobrino, J. A., (Ed.), *Teledetección*, 1st ed., pp. 328–331, Univ. de València Press, Valencia, Spain, 2000.

Sobrino, J. A., N. Raissouni, and Z.-L. Li, A comparative study of land surface emissivity retrieval from NOAA data, *Remote Sens. Environ.*, *75*, 256–266, 2001.

Stoll, M., Restitution de la temperature de surface par teletedection aeroportee dans le cadre de Hapex-Mobilhy, Ph.D. thesis, Paul Sabastier Univ., Toulouse, France, 1993.

---

J. C. Jiménez-Muñoz and J. A. Sobrino, Global Change Unit, Department of Thermodynamics, Faculty of Physics, University of Valencia, C/Dr. Moliner 50, 46100 Burjassot, Spain. (sobrino@uv.es;juancar.jimenez@uv.es)

J. Labed-Nachbrand and F. Nerry, GRTR/LSIIT, 5 Boulevard Sebastien Brant, 67400 Illkirch, France. (francoise.nerry@mail-grtr.u-strasbg.fr; jelila.labed-nachbrand@mail-grtr.u-strasbg.fr)